Multiplexing and switching of virtual electrodes in optoelectronic tweezers based on lithium niobate

Stefan Glaesener, Michael Esseling,* and Cornelia Denz

Institut für Angewandte Physik, Westfälische Wilhelms Universität Münster Correnstr. 2/4, 48149 Münster, Germany
**Corresponding author: m_esse04@uni-muenster.de*

Received April 5, 2012; revised July 2, 2012; accepted August 1, 2012;
posted August 1, 2012 (Doc. ID 166109); published September 5, 2012

We introduce a method for trapping and arranging microparticles in arbitrary two-dimensional patterns with high flexibility. For this purpose, optoelectronic tweezers based on lithium niobate as photoconductor are used to create virtual electrodes through modulated illumination. The evolving field gradients arrange microparticles due to dielectrophoretic (DEP) forces and enable an all-optical approach for DEP. In order to increase flexibility further, we investigate multiplexed electrode structures for *in situ* reconfiguration of particle arrangements. Using the all-optical erasure of previously written virtual electrodes, we demonstrate electrode switching and sequential particle trapping in a microchannel for microfluidic applications.

OCIS codes: 350.4855, 190.5330, 090.1995.

Since the 1980s optical tweezers have become one of the most promising tools to transport and rotate single particles with high accuracy and flexibility, often built as holographic optical tweezers capable of controlling some hundred particles [1,2]. Ever since their invention, these all-optical methods had to compete with electrokinetic approaches that achieve even higher throughput but generally lack flexibility [3,4]. Electrokinetics are in general related to larger trapping forces and thus smaller powers are sufficient for device operation [5]. The term electrokinetics includes a couple of effects that are able to manipulate particles on the micro- and nanoscale. Dielectrophoresis (DEP), for example, describes the interaction of uncharged particles with an electric field gradient through induced multipole moments. Both high particle throughput and the possibility to act on neutral particles, make DEP a powerful tool for analyzing and sorting devices, e.g., for cells [6]. One of the main drawbacks of these devices is a fixed electrode configuration, which limits their application to predesigned structures. In order to ensure flexible switching, optoelectronic tweezers (OET), combining optical and electrokinetic methods, have been developed [7]. In principal, OET consist of a photoconductor that allows optically controlled creation of virtual electrodes through light illumination [8]. These devices typically need an external voltage supply that counters miniaturization. Recently other photoconductors have been investigated to overcome this disadvantage, among them lithium niobate (LN)—a photorefractive material dominated by the bulk photovoltaic effect—which is capable of producing highly modulated electric fields solely through inhomogeneous illumination and is therefore a promising material for mobile OET [9–13]. In this Letter, we use as-grown LN crystals for the sequential induction and erasure of internal fields. As-grown LN possesses dark storage times in the range of weeks or months, consequently, virtual electrodes will remain permanent even if the illumination is switched off. We exploit this long storage time to create complex electrode configurations with simple light patterns imaged onto different locations of the crystal. This approach is in the following referred to as spatial multiplexing, very similar to but not to be confused with techniques of phase-code or angular multiplexing that enable the independent sequential storage and readout of information from holographic data storages [14,15]. Particle manipulation for OET based on LN crystals is achieved using DEP forces, which acting on a homogeneous dielectric bead with radius r in a surrounding medium with dielectric constant ε_m, can be described as

$$F_{\mathrm{DEP}} = 2\pi r^3 \varepsilon_m \alpha(\omega) \nabla E^2, \tag{1}$$

where $\alpha(\omega)$ is the Clausius–Mossotti factor [3]. In the low-frequency regime of the electric field, as it is the case for as-grown crystals with switching times in the range of minutes, the Clausius–Mossotti factor depends only on the conductivities $\sigma_{p/m}$ of particles (p) and medium (m)

$$\alpha(\omega \to 0) \approx \frac{\sigma_p - \sigma_m}{\sigma_p + 2\sigma_m}. \tag{2}$$

For demonstration of our concept, glassy carbon particles (Sigma-Aldrich, $\varnothing = 2 - 12\ \mu$m) and homemade graphite particles ($\varnothing = 5 - 20\ \mu$m) were dispersed in tetradecane, an unpolar nonconducting solvent. Following Eq. (2), the Clausius–Mossotti factor for these cases can be approximated by $\alpha \approx 1$ and the force acting on the microparticles only depends on the gradient of the electric field squared ∇E^2 created on the crystal surface.

In order to quantify these field inhomogeneities, the induced electric fields were measured using digital holography [13,16,17]. Through Pockels' effect, the internal space-charge field E_{SC} modifies the refractive index $\Delta n = -\frac{1}{2} n_o^3 r_{13} E_{\mathrm{SC}}$, where $n_o = 2.286$ is the unmodified refractive index for ordinary polarized readout light of wavelength $\lambda = 632.8$ nm and $r_{13} = 9.6\ \mathrm{pm\,V^{-1}}$ the corresponding electro-optic coefficient [18]. Relative phase differences $\Delta\phi(x, y)$ of the light being transmitted through the crystal of thickness $d = 500\ \mu$m can be used to calculate the spatially resolved electric field

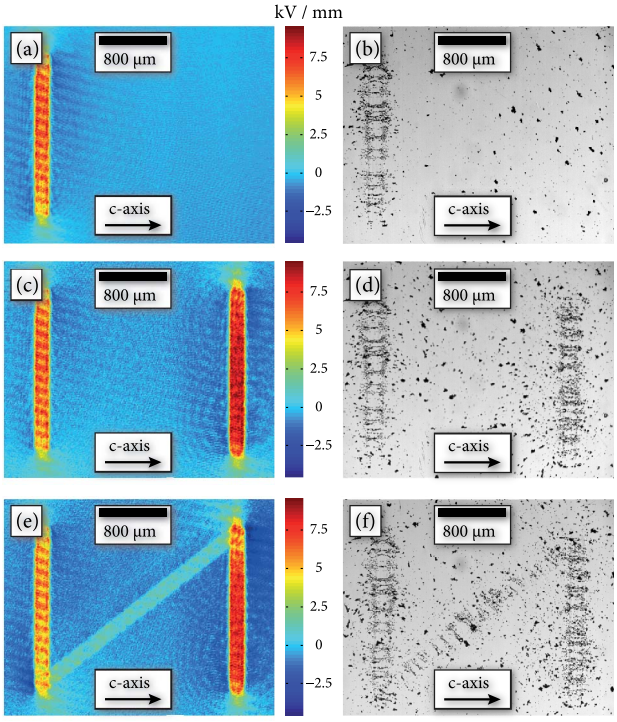

Fig. 1. (Color online) Internal electric field E_{SC} in LN measured by digital holography (a), (c), (e) and respective particle trapping (glassy carbon) (b), (d), (f). For further details refer to text.

$$E_{SC}(x,y) = -\frac{\lambda}{\pi d n_o^3 r_{13}} \Delta\phi(x,y). \tag{3}$$

In Fig. 1 we demonstrate the sequential large-scale induction of high field gradients [(a),(c),(e)] and the respective trapping patterns [(b),(d),(f)] in a three-step multiplexed configuration. For this purpose a binary stripe-shaped light field with an intensity of $I = 2.87\ \mathrm{mW\,mm^{-2}}$, created by an amplitude spatial light modulator (ASLM), is used to sequentially induce virtual electrodes by varying the modulation on the ASLM. As the generation of space-charge fields in LN is based on the photovoltaic effect, charge separation and electric field gradients along the c-axis are much stronger than those perpendicular to it. Consequently, electrode edges perpendicular to the c-axis result in larger DEP trapping forces [19]. The writing time for the different electrodes was adjusted according to their angle with the c-axis; for the 90°electrodes it has been set to $t_1 = 60$ s and $t_2 = \sqrt{2}t_1 \approx 85$ s for the 45°-electrode.

In order to observe sequential particle trapping, a reservoir, produced by polydimethylsiloxane (PDMS) replica molding [20] with subsequent UV/ozone treatment is applied to the crystal surface and filled with a suspension of tetradecane/glassy carbon. The UV/ozone treatment helps to prevent the diffusion of nonpolar solvents into the bulk PDMS [21]. The first virtual electrode is created during particle sedimentation, thus sedimenting particles in the fluid volume are influenced by the evolving field gradients and trapped at the electrode edges [Fig. 1(b)]. When writing further electrodes, particle reorganization is inhibited due to friction and adhesion to the crystal surface. However, by increasing the fluid flow with a pipette, adhered particles are dispersed again and are attracted by the newly created field gradients. As expected from the anisotropy of the photovoltaic effect, particle trapping due to electrodes including an angle different of 90° to the c-axis is less pronounced as can be seen in Fig. 1(f). In addition, pearl chain formation in the gap of two facing electrode edges —a typical effect for DEP driven particle manipulation— can be observed [22]. In principle such trapping patterns can be scaled down to the wavelength of the light. However, for the DEP force calculation, the Rayleigh approximation must hold, which means that $d_{\mathrm{particle}} \ll d_{\mathrm{electrode}}$, limiting the resolution of virtual electrodes in practical applications. Typical applications for such a trapping scheme can be found in the field of microfluidics, where selective trapping of matter out of a microfluidic stream is an everyday challenge. In this geometry a controllable fluid flow occurs naturally and adhesion can easily be overcome. To this end, the active crystal surface was integrated in a PDMS microchannel, which was actuated by a micropump pumping a suspension of graphite flakes in tetradecane through the channel ($v \approx 10\ \mu\mathrm{Ls}^{-1}$). In order to demonstrate that electrode systems cannot just be multiplexed but that switching is possible as well, we established an erasure process between two writing steps. After structured illumination with an intensity of $I = 2.5\ \mathrm{mW/mm^2}$ (measured before the sample) for four minutes using a light pattern consisting of a three-period sinusoidal grating of period $\Lambda = 200\ \mu$m and the alignment of particles, the pattern is erased by illuminating the crystal for 6 min with a homogeneous incoherent light source. Subsequently, a second electrode writing process with an angle of 45° is performed. Note that the time constants depend inversely on the light powers reaching the sample, i.e., due to losses the writing time is longer than in Fig. 1. Due to the 45° angle of the electrode with respect to the c-axis, the trapping efficiency in the second configuration is reduced compared to the first one. However, Figs. 2(b)–2(d) show that due to the erasure process electrodes and corresponding particle arrangements can be partially removed and switched. The number of switching processes is only limited by time because more and more particles stick to the channel walls, which reduces the trapping contrast. A possible explanation for this increased sticking to the walls is the presence of polar groups on the PDMS surface introduced during the UV/ozone-treatment [23]. These polar groups, which are not electrically screened by the nonpolar tetradecane, may be responsible for an increased adhesion of particles. Yet, with increased laser power and/or a more photoconductive crystal, experiments can be carried out in shorter time frames, so adhesion to the channel walls should not be a problem.

In conclusion, we demonstrated the flexible induction of multiplexed structures on LN for the use as OET. In order to characterize the flexibility of the driving force for micromanipulation, we first investigated two-dimensional electric field distributions in the crystal by the use of digital holographic methods. This allows correlating particle trapping positions with the electric field. We demonstrated that complex electrode structures can be easily created by the use of simple illumination

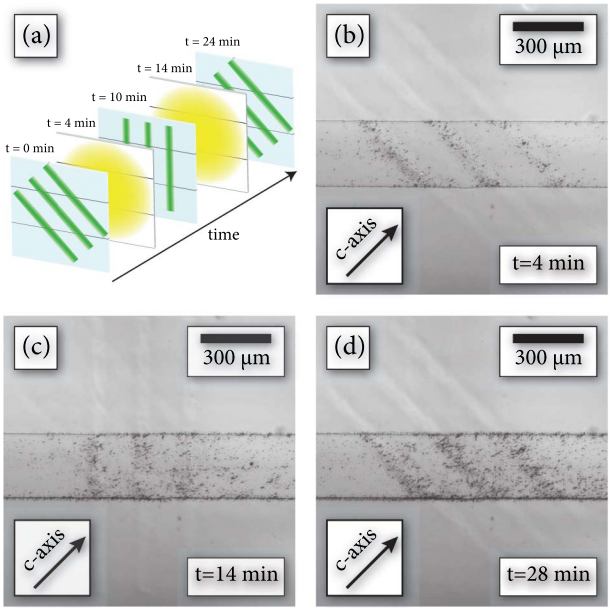

Fig. 2. (Color online) Sequential switching of virtual electrodes in order to trap graphite particles in a microchannel: (a) Illustration of the writing and erasure sequence (including time scale) and (b)–(d) corresponding particle arrangements.

patterns for temporal multiplexing. Concerning the time scale of the device, we are limited by the time constant of the LN crystal, which is determined by its photoconductivity. For future applications, this figure-of-merit can be improved by optimizing the concentration and reduction degree of doping impurities of the crystal [24], which can possibly reduce writing times by orders of magnitude. It has been demonstrated that all-optical switching of trapping patterns can be accomplished *in situ* in a microchannel. Therefore, we are convinced that time-resolved electrode reconfiguration offers an innovative solution for particle manipulation from the millimeter down to the micro- and nanometer scale.

Financial support from the German Research Foundation (Grant TRR61) is gratefully acknowledged.

References

1. A. Ashkin, J. M. Dziedzic, J. E. Bjorkholm, and S. Chu, Opt. Lett. **11**, 288 (1986).
2. D. G. Grier, Nature **424**, 810 (2003).
3. H. Pohl, J. Appl. Phys. **29**, 1182 (1958).
4. R. Pethig, Biomicrofluidics **4**, 022811 (2010).
5. T. Schnelle, T. Müller, G. Gradl, S. Shirley, and G. Fuhr, J. Electrost. **47**, 121 (1999).
6. M. del Carmen Jaramillo, E. Torrents, R. Martinez-Duarte, M. J. Madou, and A. Juarez, Electrophoresis **31**, 2921 (2010).
7. P. Chiou, A. Ohta, and M. Wu, Nature **436**, 370 (2005).
8. M. C. Wu, Nature Photon. **5**, 322 (2011).
9. H. A. Eggert, F. Y. Kuhnert, K. Buse, J. R. Adleman, and D. Psaltis, Appl. Phys. Lett. **90**, 241909 (2007).
10. X. Zhang, J. Wang, B. Tang, X. Tan, R. A. Rupp, L. Pan, Y. Kong, Q. Sun, and J. Xu, Opt. Express **17**, 9981 (2009).
11. M. Esseling, F. Holtmann, M. Woerdemann, and C. Denz, Opt. Express **18**, 17404 (2010).
12. S. Grilli and P. Ferraro, Appl. Phys. Lett. **92**, 232902 (2008).
13. L. Miccio, M. Paturzo, A. Finizio, and P. Ferraro, Opt. Express **18**, 10947 (2010).
14. C. Denz, G. Pauliat, G. Roosen, and T. Tschudi, Opt. Commun. **85**, 171 (1991).
15. K. Buse, A. Adibi, and D. Psaltis, Nature **393**, 665 (1998).
16. M. de Angelis, S. De Nicola, A. Finizio, G. Pierattini, P. Ferraro, S. Pelli, G. Righini, and S. Sebastiani, Appl. Phys. Lett. **88**, 111114 (2006).
17. M. Esseling, S. Glasener, F. Volonteri, and C. Denz, Appl. Phys. Lett. **100**, 161903 (2012).
18. P. Yeh, *Introduction to Photorefractive Nonlinear Optics* (Wiley Interscience, 1993).
19. B. Sturman and V. Fridkin, *The Photovoltaic and Photorefractive Effects in Noncentrosymmetric Materials* (Gordon & Breach Science Publishers, 1992).
20. D. C. Duffy, J. C. McDonald, O. J. A. Schueller, and G. M. Whitesides, Anal. Chem. **70**, 4974 (1998).
21. Y. Berdichevsky, J. Khandurina, A. Guttman, and Y. Lo, Sens. Actuators B **97**, 402 (2004).
22. R. Kretschmer and W. Fritzsche, Langmuir **20**, 11797 (2004).
23. S.-K. Chae, C.-H. Lee, S. H. Lee, T.-S. Kim, and J. Y. Kang, Lab Chip **9**, 1957 (2009).
24. R. Sommerfeldt, L. Holtmann, E. Krätzig, and B. Grabmeier, Phys. Status Solidi A **106**, 89 (1988).